Throughput performance of local 5G downlink in SU-MIMO under outdoor environments

Hiroki Urasawa† Hayato Soya‡ Kazuhiro Yamaguchi‡ and Hideaki Matsue†

†Guraduate school of Suwa University of Science ‡Suwa University of Science

†, ‡ 5000-1,Toyohira,Chino,Nagano,391-0292,Japan

E-mail: †gh22504@ed.sus.ac.jp,matsue@rs.sus.ac.jp ‡{soya_hayato, yamaguchi}@rs.sus.ac.jp

***Abstract*— We evaluated the throughput performance, including received power, in 4×4 single-user multiple-input multiple-output (SU-MIMO) transmission for synchronous time division duplex (TDD) and downlink data channels in comparison with single-input single-output (SISO) transmission in an environment where a local 5G wireless base station was installed on the roof of a research building at our university. After showing a simulation method for evaluating throughput characteristics in MIMO, we compared the results with experimental results. The cumulative distribution function (CDF) of the transmission throughput shows that, at a CDF of 50%, in SISO transmission, the simulated value is approximately 115 Mbps, and the experimental value is 105 Mbps, within a difference of approximately 10 Mbps. By contrast, in MIMO transmission, the simulation value is 380 Mbps, and the experimental value is approximately 420 Mbps, which is a difference of approximately 40 Mbps. It was shown that the transmission throughput characteristics can be predicted with sufficient accuracy by obtaining the delay profile and the system model at each reception point using the both ray tracing and MIMO simulation methods in actual environments.**

Keywords*— local 5G, received power characteristics, transmission throughput characteristics, ray tracing method, error vector magnitude (EVM), synchronous TDD, SISO transmitssion, SU-MIMO transmission

I. INTRODUCTION

A local 5G system[1][2] has been launched that enables local governments and companies to deploy self-employed 5G services as spot services in areas, such as private land and indoors. The Sub-6 and 28 GHz bands, which are the frequency bands of the local 5G system, were granted in 2019[3], and new bands were added in the following year, making their outdoor use possible[4]. In addition to the enhancement of these systems, at the beginning of the service, the network configuration was mainly non-standalone (NSA) architecture, which assumes a coordinated operation of 5G/4G systems. Standalone (SA) configuration has become a major advantage in terms of operation and cost. Therefore, each organization is actively deploying the system, and there is increasing development of new services for technical demonstrations and solutions to regional issues[5][6]. Based on these happenings, we considered equally introducing a local 5G system at our university.

Specifically, for a local 5G system based on the 3GPP Release 15 specifications, computer simulations have been conducted to determine system configuration, including the location and installation of wireless base station antennas, assuming outdoor use, and antenna radiation patterns.

In the past, after simulating the received power distribution using the ray tracing method[7] and comparing it with experimental results, the throughput in multiple-input multiple-output (MIMO) transmission was calculated from Shannon's theoretical formula[8][9]. Also, an example showing throughput characteristics from experimental results has been reported[10]. However, there has been no report on quantitative evaluation of the difference between the calculated value and the experimental value. Also, in the development and demonstration project for local 5G, there are multiple examples of evaluating the throughput versus received power characteristics in MIMO through experiments, but no consideration has been given to the difference between the theoretical values and the experimental values[5][6].

In this study, we first show the received power characteristics in this service area by simulation using the ray tracing method and experiment. After that, we quantitatively evaluate the difference between the theoretical value and the experimental value for the throughput versus received power characteristic in single-input single-output (SISO) transmission. Then, using the results, we show how to calculate the throughput by simulation in single-user multiple-input multiple-output (SU-MIMO) transmission, and compare the simulation values with the experimental values to confirm that the results are in good agreement. Therefore, we show the validity of the throughput simulation method in MIMO transmission under outdoor environments.

II. EVALUTION OF DOWNLINK PROPAGATION CHARACTTERRISTICS

2.1. Simulation evaluation

Table 1 lists the specifications for the simulation of radio wave downlink propagation. We used the ray tracing method as an algorithm[7][11]. The service area was assumed to be 230 m × 330 m, centered on the wireless base station, and the number of sample points was 10^4, divided into 10^2 vertically and horizontally.

At a certain reception point, if the received power of each component in the delay profile is p_i, the total received power P is expressed as follows[11][12].

$$P = \sum_{i} p_i \tag{1}$$

Figure 1 shows an example of the delay profile at a certain reception point with line-of sight (LOS) propagation. Here, through simulations and experiments, the received power is measured using a synchronization signal block (SSB) and evaluated using the reference signal received power (RSRP)[1].

Table 1. Specifications of radio wave propagation simulation

Item	Value
Algorithm	Ray tracing method
Frequency	4.8–4.9 GHz
Bandwidth	100 MHz
MIMO structure	4 transmitting, 4 receiving
Base station antenna spacing	50 cm
Base station antenna height	22.04 m (rooftop height 3 m)
Base station antenna radiation pattern	85° (horizontal plane) 60° (vertical plane)
Base station antenna tilt angle	10°
Transmission power	West side:0.2 W / antenna East side:0.12 W / antenna
Base station antenna gain	9 dBi
Receiver antenna height	1.5 m
Receiver antenna gain	2 dBi
Maximum number of reflections	3 times
Maximum number of diffractions	2 times

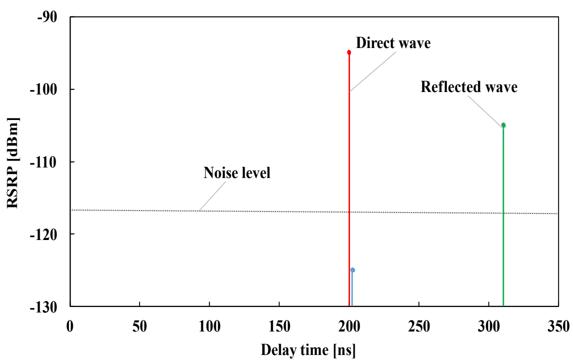

Fig.1. An example of a delay profile for LOS propagation

Figure 2 shows the simulation results for the received power obtained from the delay profile of 10^4 points using Equation (1). In Figure 2, colors inside the 32 point circle (◯) marks indicate the experimental values, and all other points indicate the simulation values. Experimental values will be described in Section 2.2. The received power directly under the base station antennas is very high, approximately −75 dBm, and approximately −90 dBm at relatively long-distance locations with visibility.

Conversely, in areas shielded by buildings, the values were as low as −110–−120 dBm. Calculating from the noise power of the wireless terminal that is the receiver: N_R = kTBF, N_R = −117 dBm assuming the noise figure of the receiver: F = 12 dB, where T is the absolute temperature inside the receiver and B is the signal bandwidth. From this result, it was confirmed that many places are below the noise level of −117 dBm.

2.2. Comparison of experimental and simulation evaluations of received power

Figure 2 shows experimental results. The experimental value of the received power is the color inside the ◯ mark at 32 points measured using the SSB signal together with the simulation results of received power discussed in Section 2.1(1). The color in the circle indicates the experimental value, and the color just outside the circle indicates the simulated value. Comparing the experimental and simulation results, received power are both extremely high at −75–−85 dBm directly under the base station antennas. Conversely, they are low at −110–−120 dBm in areas shielded by buildings. Additionally, a medium value of approximately −90 dBm is obtained at a relatively long distance of approximately 150–190 m. The measurement limit value in this experiment is obtained at approximately −117 dBm, which is the noise power of the receiver. We confirmed the validity of the simulation by demonstrating that the difference between the simulation and experimental results was within a maximum of approximately 10 dB.

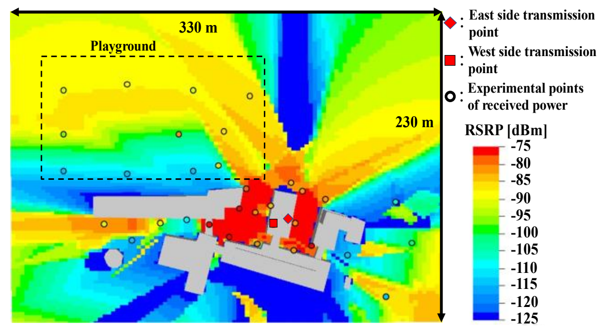

Fig.2. Comparison of simulated and experimental RSRP in the area

III. Evalution of Downlink Data Channel Transmission Throughput Characteristics

3.1. SISO transmission

(1) Theoretical examination

Table 2 lists the main specifications of the local 5G downlink data channel. The MIMO configuration was SU-MIMO, and the number of layers could be switched between one and four. First, we evaluated the characteristics of SISO with one layer. Modulation and coding scheme (MCS) configuration conforms to 3GPP TS38.214-Table 5.1.3.1-1[13][14] and dynamically controls a total of 29 combinations of modulation schemes and forward error correction coding rates.

Figure 3 shows the configuration of the local 5G network installed on campus. To evaluate the transmission throughput characteristics of the wireless part, the server was connected to the N6 interface directly below the user plane function (UPF) in the 5G core, and the open-source software LibreSpeed was installed[15]. On the other hand, the wireless terminal user equipment (UE) and notebook PC are connected by 1000 Base-T, and the transmission throughput is evaluated between this notebook PC and the server on which the LibreSpeed is installed.

Therefore, the librespeed server is connected to the PC via a UPF, radio base station (gNB), and the UE.

Here, we theoretically examine the transmission throughput of SISO transmission.

The transmission throughput of SISO transmission is obtained by the following formula[13][14].

$$\text{Throughput}_{SISO} = N \times N_{Mod} \times f \times R \times (N_{RB} \times N^{RB}{}_{SC}/T_{symbol}) \times (1-R_{OH}) \times R_{DL/(UL+DL)} \quad (2)$$

where N is the number of layers, which was set to one. N_{Mod}: Modulation order with three stages: QPSK=2, 16QAM=4, and 64QAM=6. f: Efficiency due to UE processing performance, f = 0.75 considering the amount of reference signal. R: Code rate of LDPC code. N_{RB}: Number of resource blocks (RB), 273 to use the entire 100 MHz band, $N_{RB}{}^{SC}$: Number of subcarriers per RB = 12. T_{symbol}: Time symbol length = 33.3 µs + 2.3 µs. R_{OH}: Overhead:0.14 Sub-6, $R_{DL/(UL+DL)}$: DL/(UL+DL) in the synchronous TDD was set to 7/10, considering switching slots. The required carrier-to-noise ratio (C/N) of the system corresponding to each MCS value was evaluated with reference to the value provided in 3GPP TS 38.306 4.1.2. Also, from the received noise power N_R = −117 dBm, the required received power Pr = −117 + C/N [dBm] is obtained from the required carrier-to-noise ratio (C/N), and the transmission throughput is obtained by Equation (2). Theoretical value shown in Figure 4 shows theoretical value of transmission throughput versus received power (Pr : RSRP) characteristics. Here, the vertical axis of Figure 4 indicates the throughput value calculated by Equation (2). In addition, the horizontal axis in Figure 4 corresponds to the required C/N value corresponding to the MCSindex used on the vertical axis obtained from the BER versus C/N characteristics of the 5G system[13][16]. The relationship between C/N and received power Pr, Pr = −117 + C/N. The transmission throughput increased as the received power increased. For example, the transmission throughput is approximately 50 Mbps at the received power of −112 dBm, and approximately 230 Mbps at the received power of −97 dBm.

Table 2. Specifications of the local 5G downlink data channel

Item	Value
Frequency	4.8–4.9 GHz
Channel bandwidth	100 MHz
MIMO structure and number of layers	SU-MIMO 1(SISO), 4(MIMO)
Base station antenna spacing	50 cm
MCS structure	MCS Index: 0–28
Modulation scheme	OFDM Primary modulation QPSK/16QAM/64QAM
Forward error correction codes	LDPC, Rate 0.117–0.925
Subcarrier spacing	30 kHz
OFDM symbol length CP length	33.3 µs 2.3 µs
DL : UL ratio for synchronization TDD	7 : 2

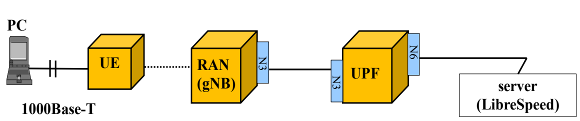

Fig.3. Network configuration when measuring transmission throughout

(2) Experimental results

In the throughput measurement experiment, the measurement time by Librespeed was set to 30 seconds at each measurement point, and the average value was measured five times, and the average value was used as the experimental value. The amount of variation varied depending on the measurement points, and the variation of the measured values tended to be large especially at the nonline-of-sight (NLOS) points.

Figure 4 shows the theoretical values of the transmission throughput versus the received power characteristics and the experimental results of the transmission throughput at the same 32 points discussed in Section 2.1.

In the experimental results, line-of-sight (LOS) propagation is indicated by ● marks, and nonline-of-sight (NLOS) propagation is indicated by × marks. In comparing the theoretical and experimental values of the transmission throughput, we consider three regions according to the value of the received power: received power is less than −110 dBm, ranges from −110–−100 dBm, and is more than −100 dBm.

There are 5 points that greatly deviate upward from the theoretical value, and 1 point that greatly deviates downward from the theoretical value. At the other 4 points, it is 60–80 Mbps, which is a value close to the theoretical value.

Next, in the medium received power range of −110–−100 dBm, the transmission throughput gradually deviates from the theoretical value and decreases to approximately 80–110 Mbps. At a high received power of −100 dBm or more, it can be confirmed that the transmission throughput saturated at a nearly constant value of 110–130 Mbps in this power range, except for a few singular values.

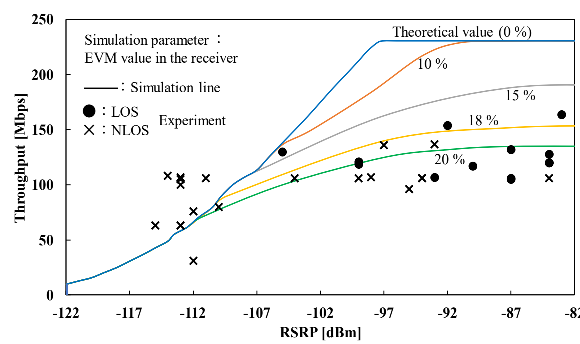

Fig. 4. Transmission throughput versus RSRP characteristics in SISO (Simulation parameter: EVM value in the receiver)

(3) Consideration of experimental results

In analyzing the factors that significantly reduce the transmission throughput from the theoretical value, the following three causes can be considered.

Cause 1: Error vector magnitude (EVM) increases due to multipath fading.

Cause 2: EVM increases due to interference from other systems.

Cause 3: EVM increases due to interference in receiver.

First, let us consider cause 1. Figure 4 also shows the simulation results of the transmission throughput versus received power characteristics when the value of the residual

EVM in the receiver was set to 0% (theoretical value), 10%, 15%, 18%, and 20%. If $EVM_{\%}$ is converted to EVM_{dB} and expressed as the carrier-to-interference ratio (C/I), the C/N value is C/(N+I) by adding the residual EVM value. For example, $EVM_{\%} = 20\%$ corresponds to $EVM_{dB} = 14$ dB[17]. Therefore, C/(N+I) will saturate at 14dB. As a result, the throughput value decreases when the residual EVM value is present. The transmission throughput of the simulation result when EVM value is 18–20% and the transmission throughput of the experimental result are in good agreement.

Regarding cause 2, interference from other systems, there is currently only one wireless base station in operation, and we have confirmed that there is no interference on the same frequency in the surrounding area; therefore, we do not believe that cause 2 will be a factor.

Finally, for cause 3, Regarding interference within the receiver, interference from the Wi-Fi that exists within the receiver can be considered. However, it is thought that the impact will be negligible.

Based on these considerations, the main cause of transmission throughput degradation is an increase in the EVM value in the receiver, which is significantly affected by multipath fading in the propagation path.

3.2. MIMO transmission

(1) Simulation evaluation

In MIMO transmission, the transmission throughput can be increased by actively utilizing a multipath environment. The MIMO operation is considered below.

When the transmitted signal vector $\tilde{x}$, received signal vector r, noise signal vector n, and channel response matrix H are combined, the received signal vector r is expressed as follows:

$$r = H\tilde{x} + n \tag{3}$$

Next, the singular value decomposition of the channel response matrix H is performed.

$$H = U\Sigma V^H \tag{4}$$

$$\Sigma \equiv \mathrm{diag}(\sqrt{\lambda_1}\sqrt{\lambda_2} \cdots \sqrt{\lambda_m}) \tag{5}$$

Consequently, the channel can be orthogonalized using the right singular vector V as the transmission weight and the left singular value vector U^H as the reception weight. where m is the number of transmitting antennas or receiving antennas, whichever is smaller than.

Therefore, the eigen beam of the transmitted signal vector $\tilde{x}$ is the information signal x multiplied by V.

$$\tilde{x} = Vx \tag{6}$$

The result is as follows.

By contrast, the separation of the information signal y at the receiving side is obtained by multiplying the received signal vector r by U^H.

$$y = U^H r = U^H HVx + U^H n = U^H U\Sigma V^H Vx + U^H n$$
$$= \Sigma x + U^H n \tag{7}$$

Subsequently, MIMO channels can be orthogonalized to independent channels, and eigenmode transmission can be performed without interference from other eigenpaths [18][19]. Figure 5 shows an eigenmode 4×4 MIMO system configuration.

A channel model used in throughput simulations in 4×4 SU-MIMO is described. Regarding the delay profile characteristics of 32 points obtained by ray tracing method as described in Section 2.1. Figure 1 is an example of a delay profile due to LOS propagation, showing the presence of direct wave and reflected wave. We assumed Rician fading at LOS propagation points as described in the 3GPP channel model TDL-D[20]. On the other hand, at NLOS propagation points, we assumed Rayleigh fading as described in the 3GPP channel model TDL-C[20]. The K-factor in Rician fading is as a ratio of received power of the direct wave and the sum of received power of the multiple reflected and/or the diffracted waves. Reflected and diffracted waves in the delay profile are assumed to be Rayleigh fading because they are NLOS propagation, and each wave is assumed to fluctuate independently[20].

Assuming that the propagation path slowly fluctuates, the Doppler frequency is 0.5 Hz and the number of samples is 50000.

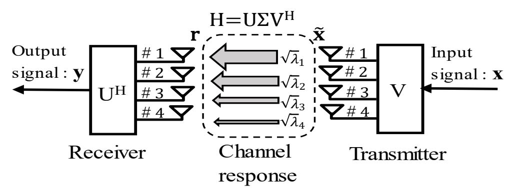

Fig. 5. Eigenmode 4 × 4 MIMO system configuration

The simulated transmission throughput characteristics of 4×4 MIMO were derived from the channel model. Figure 6 shows the simulation results of the eigenvalue-to-noise power ratio distribution in the eigenmode transmission of a 4×4 MIMO system. Probability density function of the first eigenvalue-to-noise power ratio $\mathrm{prob}_{\lambda 1}$ is distributed at the center value of approximately 27 dB. Similarly, probability density function of the second eigenvalue-to-noise power ratio $\mathrm{prob}_{\lambda 2}$, probability density function of the third eigenvalue-to-noise power ratio $\mathrm{prob}_{\lambda 3}$, and probability density function of the fourth eigenvalue-to-noise power ratio $\mathrm{prob}_{\lambda 4}$, have central values of approximately 23, 19, and 12 dB, respectively.

As a simulation evaluation method of throughput by MIMO, it is assumed that the simulation characteristics of throughput versus received power in SISO transmission obtained earlier are the same as the characteristics of SISO transmission for each of the four layers in MIMO transmission. Then, the throughput in 4×4 MIMO transmission is obtained by summing the throughput of the four layers from the two results of the probability density function of the eigenvalue versus noise power ratio shown in Figure 6 and the throughput versus received power characteristics in SISO transmission shown in characteristics of EVM = 20% in Figure 4. Expressed as a formula, it becomes the following formula.

$$\text{Throughput}_{4\times4\text{MIMO}} = \sum_{i=1}^{4}\int_{0}^{\infty} \text{prob}_{\lambda i}(\gamma) \times \text{throughput}(\gamma)d\gamma \qquad (8)$$

Where γ is the antilogarithm of C/N [dB], as a result, $\gamma = 10^{C/N/10}$, and $\text{prob}_{\lambda i}$ is the probability density function of the i-th eigenvalue-to-noise power ratio (i = 1,…,4). Where $\int_0^{\infty} \text{prob}_{\lambda i}(\gamma)d\gamma = 1$, $\text{throughput}(\gamma)$ shows the simulation results of throughput versus C/N characteristics with EVM = 20% value in Figure 4. Here, the received power in Figure 4 is represented by C/N + noise power of −117 dBm.

Details are given below. In this example, the maximum throughput of 120 Mbps is obtained from the first eigenvalue and the second eigenvalue from Figures 6. Approximately 110 Mbps is obtained from the third eigenvalue, and approximately 80 Mbps is obtained from the fourth eigenvalue, for a total of 430 Mbps. Similarly, simulation results of throughput in MIMO for a total of 32 points are obtained and shown in Figure 7.

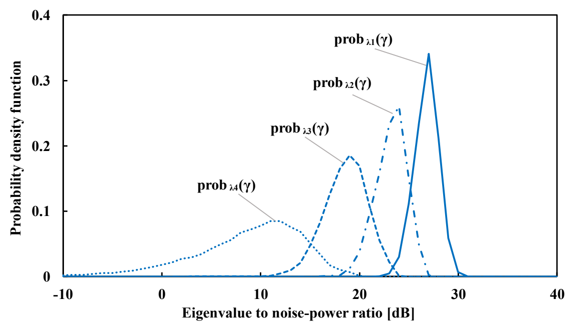

Fig.6. An example of probability decsity funcyion of eigenvalue to noise power ratio

(2) Comparison of experimental and simulation results

Figure 7 compares the simulation results and experimental results of transmission throughput values at 32 points. The simulation results are shown in the color inside the △ marks, and the experimental results are shown in the color inside the ○ marks. The results indicate that the difference between simulation and experimental values was within 100 Mbps, which is a relatively close correspondence. However, at some points surrounded by buildings, the experimental value was 100 Mbps higher than the simulation value. This may be because the position and height of the buildings in the simulation differed slightly from those in the actual environment.

Based on the results in Figures 4 and 7, Figure 8 shows the transmission throughput versus the received power characteristics of the simulations and experiments in SISO and MIMO transmission. Here, the simulated and experimental values of SISO in Figure 8 are the simulated values of EVM = 20% and experimental value in Figure 4. As for the MIMO throughput value, the results of Figure 8 are used for simulation and experimental values. As for the received power, the results of Figure 2 are used for simulation and experimental values. They are collectively displayed in Figure 8. Of the experimental values, ● marks indicate LOS propagation, × marks indicate NLOS propagation, and △marks indicate simulation values. In MIMO transmission, as in SISO transmission, as the received power increases, the transmission throughput increases correspondingly. In addition, there are points where the transmission throughput decreases even if the received power is high. This is because the delay spread value is relatively small; therefore, a sufficiently large transmission throughput could not be obtained. Furthermore, it was shown that there was no significant difference in the effects of NLOS and LOS propagation on the transmission throughput.

Figure 9 shows the cumulative distribution function characteristics of the transmission throughput obtained from the results shown in Figure 8. As indicated, for SISO and MIMO, the trends in the distributions of the simulation and experimental values agreed closely. For example, at a CDF of 50%, the simulation value for SISO transmission was approximately 115 Mbps and the experimental value was 105 Mbps, giving a difference of approximately 10 Mbps. However, in MIMO transmission, the simulation value was approximately 380 Mbps, and the experimental value was approximately 420 Mbps, which is a difference of approximately 40 Mbps.

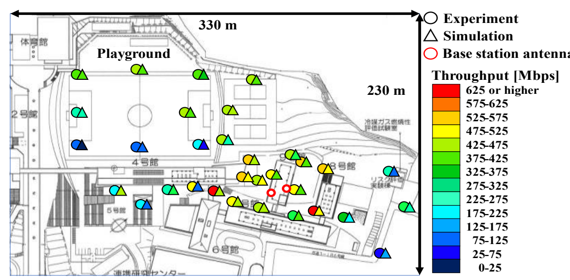

Fig. 7. Comparison of simulated and experimental results of MIMO transmission throughput in the area

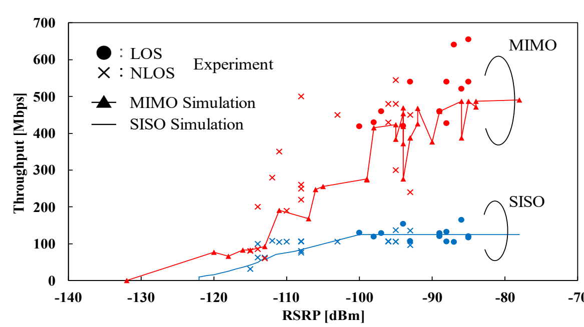

Fig. 8. Comparison of simulated and experimental results for transmission throughput versus RSRP in SISO and MIMO transmission

IV. Conclusion

In an environment where a local 5G base station antennas were installed on the roof of a research building at a university, the transmission characteristics of synchronous TDD and downlink data channel 4×4 MIMO transmissions were evaluated and compared with SISO transmission. Consequently, regarding the received power characteristics, the difference between the simulation value, which was based on the ray tracing method, and experimental value at

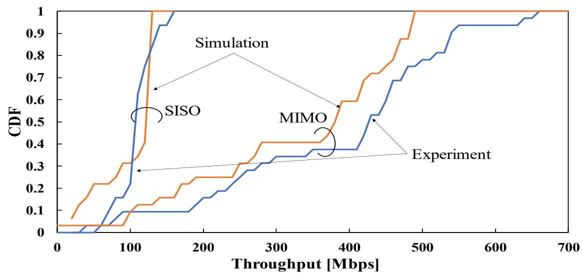

Fig.9. Cumulative distribution characteristics of simulated and experimental results of transmission throughputs in SISO and MIMO

32 points in the area was within a maximum difference of approximately 10 dB, and the simulation value at 50% of the cumulative distribution was approximately −97 dBm. This was in close agreement with the obtained experimental value of approximately −99 dBm.

Regarding the transmission throughput versus received power characteristics of SISO transmission, it was shown that the experimental and theoretical values are relatively consistent when the received power is relatively small, however as the received power increases, the experimental throughput values deviate from the theoretical values and saturate at a certain value. The cause analysis showed that the EVM value in the receiver remained at approximately 20%, owing to a large influence of multipath fading occurring in the propagation path.

Next, as a simulation evaluation method of throughput versus received power characteristics in MIMO transmission, an evaluation method based on throughput characteristics in SISO transmission was presented. As a result of comparing the simulation results obtained by this method and experimental results, the transmission throughput increases in correspondence with the received power; however, the variation in the values also increases. From the cumulative distribution of the transmission throughput value, at a CDF of 50% in SISO transmission, the simulation value was approximately 115 Mbps and the experimental value was 105 Mbps, which was within a difference of approximately 10 Mbps, because it matched both. However, in MIMO transmission, the simulation value was 380 Mbps, and the experimental value was approximately 420 Mbps, which was a difference of approximately 40 Mbps, this value is considered small enough. We clarified the effect of sufficient transmission throughput improvement in MIMO transmission. The estimated EVM value of this time was a value unique to this area, and it is necessary to examine it for each area.

From these results, it was shown that the received power and transmission throughput characteristics can be predicted with sufficient accuracy by obtaining the delay profile. Also, the effectiveness of the throughput simulation method in MIMO transmission based on SISO transmission was demonstrated under outdoor environments.

V. Acknowledgments

We would like to thank everyone involved at NEC Networks & System Integration Corporation for their cooperation in conducting this experiment.

VI. References

[1] 3GPP Release 15 TR21.915 Vol.5.0, December 2018.

[2] Chris Johnson,"5G New Radio in Bullets 1st Edition(Colour)",Chris Johnson,Farnham England, December 2022.

[3] Ministry of Internal Affairs and Communications. WHITE PAPER Information and Communications in Japan, Year 2020. [Online] Available: https://www.soumu.go.jp/johotsusintokei/whitepaper/ja/r02/pdf/n2400000.pdf

[4] Ministry of Internal Affairs and Communications. WHITE PAPER Information and Communications in Japan, Year 2021. [Online] Available: https://www.soumu.go.jp/johotsusintokei/whitepaper/ja/r03/pdf/n5600000.pdf

[5] https://www.soumu.go.jp/main_content/000712738.pdf

[6] https://www.soumu.go.jp/main_content/000813620.pdf

[7] Ch-Min LI, Dong-Lin LU, Pao-Jen WANG, "Indoor Partition Attenuations and Base Station Deployments for the 5G wireless Communications", IEICE Trans.Comm, Vol.E105–B, pp.729–736, June 2022.

[8] Ryotaro Taniguchi, Kentaro Nishimori, "Comparison of SNR and channel capacity with micro and milli-meter wave bands based on outdoor propagation measurement", IEICE Communication Express, Vol.9, No.6, pp.153-158, January 2020.

[9] Bakar Rohani, Kanata Takahashi, Hiroyuki Arai, Yasuko Kimura, Taisuke Ihara, "Improving Channel Capacity in Indoor 4×4 MIMO Base Station Utilizing Small Bidirectional Antenna", IEEE Trans. on Antennas and Propagation, Vol.66, No.1, January 2018.

[10] Yukihiko OKUMURA, Satoshi SUYAMA, Jun MASHINO, Kazushi MURAOKA, "Recent Activities of 5G Experimental Trials on Massive MIMO Technologies and 5G System Trials Toward New Services Creation", IEICE Trans.Comm, Vol.E102–B, pp.1352–1362, August 2019.

[11] Tetsuro Imai, "Mobile Radio Propagation Simulation Based on Ray-Tracing Method", IEICE Trans.Comm B, Vol.J92–B, No.9, pp.1333-1347, 2009.

[12] Goldsmith, Andrea, "Wireless Communications", Cambridge University Press, pp.86, 2005.

[13] 3GPP TS 38.214 V15.2.0,3rd Generation Partnership Project, Technical Specification Group Radio Access Network' NR Physical layer produces for data (Release15), June 2018.

[14] 3GPP TS 38.306 V4.1.2,3rd Generation Partnership project, Technical Specification Group Radio Access Network' NR Physical Layer procedures for data (Release 16), December 2019.

[15] https://github.com/librespeed/speedtest

[16] Kentaro Nishimori "On Communication Quality by Simple Evaluation Method Using 5G Signals", IEICE Technical Report, CQ2020-103, January 2021.

[17] Andreas Schwarzinger "Digital Signal Processing in Modern Communication Systems", CPSIA information can be obtained at www.ICGtesting .com Printed in the USA, pp.259, 2013.

[18] S.K.Jayaweera and H.V.Poor,"Capacity of multiple-antenna systems with both receiver and transmitter channel state information ",IEEE Trans.Inform.Theory, vol.49, no.10, pp.2697–2709, 2003.

[19] M.Lamarca,"linear precoding for mutual information maximization in MIMO systems", Inte'l Symp.Wireless Commun. Systems (ISWCS'09), pp.26–30, 2009.

[20] 3GPP TR 38.901 "Study on channel model for frequencies from 0.5 to 100 GHz," V16.0.0, October 2019.